
Masters Theses

Student Theses and Dissertations

1968

The modeling, fabrication, and testing of an instantaneous torque measuring system

Thomas Phillip Hertel

Follow this and additional works at: https://scholarsmine.mst.edu/masters_theses



Part of the [Electrical and Computer Engineering Commons](#)

Department:

Recommended Citation

Hertel, Thomas Phillip, "The modeling, fabrication, and testing of an instantaneous torque measuring system" (1968). *Masters Theses*. 7016.

https://scholarsmine.mst.edu/masters_theses/7016

This thesis is brought to you by Scholars' Mine, a service of the Missouri S&T Library and Learning Resources. This work is protected by U. S. Copyright Law. Unauthorized use including reproduction for redistribution requires the permission of the copyright holder. For more information, please contact scholarsmine@mst.edu.

THE MODELING, FABRICATION, AND TESTING OF AN
INSTANTANEOUS TORQUE MEASURING SYSTEM

BY

THOMAS PHILLIP HERTEL

A

THESIS

submitted to the faculty of

THE UNIVERSITY OF MISSOURI - ROLLA

in partial fulfillment of the requirement for the

Degree of

MASTER OF SCIENCE IN ELECTRICAL ENGINEERING

Rolla, Missouri

1968

134526

Approved by

Ralph S. Carson (advisor)

E. L. Bertnolli

R. E. Offner

ABSTRACT

The purpose of this work was to obtain a measuring system to experimentally determine the instantaneous magnitude and frequency of the torques from zero to 2400 Hertz produced by a single phase motor. This paper explains the methods employed in designing and fabricating a measuring system and shows the results from tests using this equipment. It was found that a measuring system based on the determination of the instantaneous value of the stator's reaction torques could be realized. Also, it was found that some simple methods of computation could be used to find the magnitudes of the frequency components comprising these instantaneous torques.

TABLE OF CONTENTS

	<u>Page</u>
Preface	iv
List of Figures	v
I. Introduction	1
II. Discussion of the Model of the Measuring System and Experimental Methods	3
III. Experimental Results	11
IV. Conclusions	15
Appendix A - Description of Equipment	17
Appendix B - Methods of Data Reduction used with the Baldwin-Lima-Hamilton Strain Gage and Strain Sensitivity Tables	19
Appendix C - Methods and Procedures Used in the Experimental Determination of the Constants	26
Appendix D - Computer Program for Inverse Transfer Function and Tables of Magnitude and Phase for Ten-Hertz Increments	31
Bibliography	46
Vita	47

PREFACE

The main objective of the work required in performing this research was the physical construction of a test stand to enable measurement and comparison of the magnitudes of the torque components present within the instantaneous torque produced by a single phase machine.

I wish to thank Mr. Richard Pohl, Mr. Charles Gross, Mr. Frank Huskey, Mr. Edward Hornsey, and Dr. Ralph Carson for their assistance in the design and building of this system.

LIST OF FIGURES

	<u>Page</u>
Figure 1. Picture of Complete Test Stand	38
Figure 2. Drawing of Measuring Elements	39
Figure 3. Graph of Friction Force vs. Angular Velocity	40
Figure 4. Plot of Inverse Transfer Function vs. Frequency	41
Figure 5. Picture of Responses to a Series of Impulse Loads	42
Figure 6. Drawing of the Response of a Single Phase Motor to a Load Change	43
Figure 7. Drawing of the Response of a Capacitor Split Motor to a Load Change	44
Figure 8. Temperature Coefficient of P-Type Silicon for Strain Gage	45

I. INTRODUCTION

Considerable study has been made concerning the torques and the audio frequency vibrations produced by a single phase motor. The audio frequency vibration is observed to increase whenever the motor is excited from a source controlled by non-linear devices, such as silicon controlled rectifiers. An instantaneous torque measuring system with a frequency response of zero to 2400 Hertz was required to confirm the theoretical torques produced by a single phase motor excited from a non-sinusoidal source.

Two major approaches were available in measuring these instantaneous torques: (1) to make acceleration studies of the rotor and use this data in a model for the instantaneous torques, and (2) to measure the reaction torque of the stator and use this data in a model for the instantaneous torques. There are certain advantages associated with each of the two methods; however, the reaction torque method was chosen for this work. The primary reasons for using the reaction torque method were: (1) the availability of semiconductor strain gages; (2) the ease with which different restraints and supports could be tried; and (3) the requirement of making the tests at all load conditions including no connected shaft load.

After choosing the method of measurement, a mathematical model of the measuring system was derived. This model was to represent the physical system's response to torque

with a frequency range of zero to 2400 Hertz and to aid in choosing techniques required to compensate for the system's response. Since the frequency response of the strain gage and the recorder was much higher than the natural frequency of the measuring system, their effects could be ignored. Therefore, the transfer function of the system could be approximated by the transfer function of a second-order system.

A system was then constructed using this preliminary work as a guide and the constants for a final mathematical model were experimentally measured. The system is now in use for instantaneous torque studies.

II. DISCUSSION OF THE MODEL OF THE MEASURING SYSTEM AND EXPERIMENTAL METHODS

The measurement of the instantaneous torques to 2400 Hertz by stator reaction methods required a physically stiff measuring system. After many different configurations and attachments were tried, the last approach shown in figure 1 operated best.

For any measuring system, the mathematical model of the system is required in order to convert from the measured value to a true value. The modeling of this system required several assumptions:

- (a) The reaction torque present in the stator's iron is transmitted to the measuring beam without any deflection of the stator.
- (b) The motion of the stator is very small. Therefore the moment acting on the threads in the stator is small and can be neglected. Thus the torque produced by the motor, $T_s(t)$, is represented at the base of the beam as a time-varying force, $P(t)$ times the radius of the motor, r_m .
- (c) The measuring beam is homogeneous and has the same effective cross section throughout its length, L .
- (d) The hysteresis and backlash effects of the measuring system are small and may be neglected.
- (e) The kinetic friction between the stator and the rotor is much smaller than T_s maximum.

With these assumptions, an approximate mathematical model of the transfer function of the torque measuring

system was derived.

The equation describing the reaction torque of the stator is

$$T_S(t) = J_S \ddot{\theta} + f_S \dot{\theta} + K_T \theta + C \quad (1)$$

where

$$T_S(t) = \text{reaction stator torque} = P(t)r_m$$

$$J_S = \text{mass moment of inertia of stator about the center line of the rotor}$$

$$f_S = \text{viscous friction coefficient}$$

$$K_T = \text{torsional-spring constant of the beam}$$

$$C = \text{kinetic friction}$$

$$\theta = \text{angular displacement of stator}$$

However, by applying assumption (e), the equation reduces to

$$T_S(t) = J_S \ddot{\theta} + f_S \dot{\theta} + K_T \theta \quad (2)$$

Taking the Laplace transform of equation (2) and setting all initial conditions equal to zero yields

$$T_S(s) = s^2 J_S \theta + s f_S \theta + K_T \theta \quad (3)$$

Since the measured torque, $T_o(t)$, is taken from a strain gage on the beam then

$$T_o(t) = K_T \theta \quad (4)$$

and taking the Laplace transform of equation (4) gives

$$T_o(s) = K_T \theta \quad (5)$$

So the transfer function of the system is

$$\frac{T_o(s)}{T_S(s)} = \frac{K_T \theta}{s^2 J_S \theta + s f_S \theta + K_T \theta} = \frac{K_T}{s^2 J_S + s f_S + K_T} \quad (6)$$

A picture of the beam with strain gage mounted is shown in figure 2.

From the mechanics of materials, a beam can be represented by the differential equation

$$EI\ddot{y} = M_x(t) \quad (7)$$

where

$M_x(t)$ = time varying moment at a point x

\ddot{y} = the second time derivative of the deflection y

E = modulus of elasticity of the beam

I = the centroidal moment of inertia of the beam

Then, by using the assumption made in (b), the beam is considered to be cantilevered from a fixed reference to the motor. Therefore, the solution of the differential equation

$$\ddot{y} = M_x(t)/EI \quad (8)$$

gives

$$Y = \frac{P(t)X^3}{6EI} - \frac{P(t)LX^2}{2EI} \quad (9)$$

where

$$P(t) = \frac{T_o(t)}{r_m} \quad (10)$$

and

L = length of beam

Evaluating equation (9) at $X = L$ gives

$$Y = - \frac{P(t)L^3}{3EI} \quad (11)$$

Also, from mechanics of materials

$$K_T = \frac{ft - lbs}{\text{radian}} = \frac{r_m P(t)}{\theta} \quad (12)$$

where K_T is the torsional spring constant.

But, applying the assumptions of (b) gives

$$\alpha = \frac{y}{L} \quad (13)$$

and further

$$\theta = \frac{y}{r_m} = \frac{L}{r_m} \quad (14)$$

So, substituting equation (14) into equation (12) yields

$$K_T = \frac{r_m P(t)}{\frac{y}{r_m}} = \frac{(r_m)^2 P(t)}{y} \quad (15)$$

and substituting y from equation (11) into equation (15) gives

$$K_T = \frac{(r_m)^2 P(t)}{\frac{P(t)L^3}{3EI}} = \frac{3(r_m)^2 EI}{L^3} \quad (16)$$

So for a $\frac{1}{2}$ inch by $\frac{1}{2}$ inch by $1\frac{1}{2}$ inch steel beam

$$E = 30 \times 10^6 \frac{\text{lbs}}{\text{in}^2}$$

$$I = \frac{1}{192} \text{ in}^4$$

Therefore

$$\begin{aligned} K_T &= \frac{3 \times (2.8)^2 \times 30 \times 10^6}{192 \times (1.5)^3} \\ &= 10.8 \times 10^5 \frac{\text{in} - \text{lbs}}{\text{radian}} \text{ or } 9.08 \times 10^4 \frac{\text{ft} - \text{lbs}}{\text{radian}} \end{aligned} \quad (17)$$

The value for f_s , the viscous friction coefficient, was found from figure (3), the plot of the friction force versus the angular velocity, by taking the slope of the curve times the radius of the motor.

Therefore

$$f_s = \frac{\Delta y}{\Delta x} r_m = \frac{(2.8)(0.101 - .085)}{12 \times 41.9} = 8.9 \times 10^{-5} \frac{\text{ft} - \text{lbs}}{\text{radian/sec.}} \quad (18)$$

The mass moment of inertia of the stator alone can be calculated using the weight of the stator and assuming it concentrated into a thin ring at a center of $\frac{1}{2}(r_m + r_{m_i})$ inches, where r_{m_i} is the internal radius of the motor. Adding this mass moment of inertia to twice the value of the mass moment of inertia contributed by one of the end bells, yields the mass moment of inertia, J_s , used in the model. Therefore, since the stator's weight was five pounds, the end bell's weight was $\frac{1}{2}$ pound each, r_m was 2.8 inches, and r_{m_i} was 1.6 inches, (1) then

$$J_s = \left[\frac{r_m + r_{m_i}}{2} \right]^2 \times \frac{\text{weight}}{g} + 2 \left(\frac{1}{2} r_m^2 \times \frac{\text{weight}}{g} \right) \quad (19)$$

$$= 6.95 \times 10^{-3} \text{ slug} \cdot \text{ft}^2$$

Thus the transfer function of the measuring system, equation (6) becomes

$$\frac{T_o(s)}{T_s(s)} = \frac{K_T}{s^2 J_s + s f_s + K_T} \quad (20)$$

$$= \frac{9.08 \times 10^4}{6.95 \times 10^{-3} s^2 + 8.9 \times 10^{-5} s + 9.08 \times 10^4} \quad (20a)$$

Now forming the characteristic equation

$$0 = 6.95 \times 10^{-3} s^2 + 8.9 \times 10^{-5} s + 9.08 \times 10^4 \quad (21)$$

and solving for s gives

$$s = 0.0064 \pm j3610 = \sigma + j\omega_n$$

So f_n of the system should be approximately 575 Hertz.

(1) For the complete description of the motor see Appendix A.

Now

$$\zeta = \frac{f}{2} \sqrt{\frac{1}{K_T J_S}} \quad (22)$$

and by substituting in the values of K_T , f_S , and J_S from equations (17), (18) and (19)

$$\zeta = 1.77 \times 10^{-6} \quad (22a)$$

Also the damped angular frequency, ω_d , is given by

$$\omega_d = \sqrt{1 - \zeta^2} \omega_n \quad (23)$$

So by substituting in the values of ζ and ω_n yields

$$\omega_d = \sqrt{1 - (1.77 \times 10^{-6})^2} \times 3610 \approx 3610 \text{ radian/second}$$

or

$$f_d = 575 \text{ Hertz}$$

Further modeling was required to get the torque in terms of the output voltage of a bridge.

From mechanics of materials, the relationship giving strain at point x as a function of moment at x is

$$\epsilon_x(t) = \frac{M_x(t)c}{EI} \quad (24)$$

where

c = the distance to the centroid axis to the point x

ϵ_x = the strain at x

Now since

$$M_x = P(t)(L-X) \quad (25)$$

so by substituting equation (25) into equation (24)

$$\epsilon_x(t) = \frac{P(t)(L-X)c}{EI} \quad (26)$$

For this measuring system

$$x = 1 \text{ inch}; c = \frac{1}{4} \text{ inch}$$

then by evaluating equation (26)

$$\epsilon(t) = \frac{P(t)(3/2 - 1)^{\frac{1}{4}}}{30 \times 10^0 \times 1/192} = 0.8P(t) \times 10^{-6} \frac{\text{inch}}{\text{inch}} \quad (26a)$$

But from equation (10)

$$P(t) = \frac{T_o(t)}{r_m}$$

so substituting the value of P(t) from equation (10) into equation (26a)

$$\epsilon(t) = \frac{0.8 \times T_o(t) \times 10^{-6}}{2.8} \quad (27)$$

and rearranging

$$T_o(t) = 3.50 \epsilon(t) \times 10^6 \quad (27a)$$

Since ϵ is measured as an unbalanced voltage from a bridge, than for a very small imbalance

$$E_o(t) = \frac{E_s}{2} \epsilon(t) \text{G.F.} \quad (28)$$

where

G.F. = gage factor⁽²⁾ of the strain gage

E_s = the source voltage for the bridge

E_o = the output voltage of the birdge

Thus, substituting equation (27) into equation (28) and rearranging

$$T_o(t) = \frac{7.00 E_o(t) \times 10^6}{E_s \text{G.F.}} \quad (29)$$

(2) Methods required to obtain approximate linear gage factor were taken from the Semiconductor Strain Gage Handbook, Section Two on data reduction. Baldwin-Lima-Hamilton; Waltham, Mass.

and for a gage factor of 157 and an E_s of 22-1/2 volts⁽³⁾

$$\begin{aligned} T_o(t) &= 1.99E_o(t) \times 10^3 \text{ in} - \text{lbs} \\ &= 0.166E_o(t) \times 10^3 \text{ ft} - \text{lbs} \end{aligned} \quad (30)$$

(3) See Appendix (B) for calculation of gage factor.

III. EXPERIMENTAL RESULTS⁽⁴⁾

The experimental data taken from the test stand agreed fairly well with that found from the mathematical model. However, for the real system, the assumption of no hysteresis and backlash was not completely valid. Also the low frequency torques produced by rotor imbalance and mechanical misalignment was an unexpected problem.

J_s was found experimentally to be 5.85×10^{-3} slug-ft². This compared well with the predicted value of 6.95×10^{-3} slug-ft². The difference was probably caused by the assumption that the stator could be represented by a homogeneous thin ring at an average radius. f_s was found experimentally to be 3.07 ft-lbs/radian. This value is several orders of magnitude larger than the predicted value of 8.9×10^{-5} and probably represents the effect of energy absorption within the beam, an effect that was not included in the mathematical model. Using the experimentally determined value of f_s in the calculation of the damping factor yielded a value of 0.0705, which is light damping and has very little effect on other calculations, such as ω_n the natural angular frequency. K_T was found to be 8.1×10^4 ft-lbs/radian and was near the calculated value of 9.08×10^4 ft-lbs/radian. The difference found in K_T was probably caused by the assumptions made in (b) and (c). In particular, the beam was attached to the

(4) See Appendix C for the calculations.

motor by threads tapped into the stator and cut onto the beam, then a jam nut was placed on the beam and against the motor in order to minimize the backlash. The threads cut into the beam reduced the cross-section of the resisting area of the member enough to slightly decrease K_T and thereby caused a slight decrease in ω_n . The damped natural frequency of this system was found experimentally to be 590 Hertz, by both step and impulse loading. This value happened to be very close to the calculated value because both the mass moment of inertia of the stator and the beam's stiffness decreased. The constant relating the torque to the output voltage of the bridge circuit containing the strain gage was found to be 1.23×10^3 ft - lbs/volt. This compares with the calculated value of 0.166×10^3 ft - lbs/volt. The difference is probably caused by the unpredictable stress concentration at the beam's base and the hysteresis and backlash effects in the system.

Substituting the values found experimentally into equation (6) yields

$$\frac{T_o(j\omega)}{T_s(j\omega)} = \frac{8.1 \times 10^4}{5.85 \times 10^{-3}(-\omega^2) + 3.07(j\omega) + 8.1 \times 10^4} \quad (31)$$

This equation can be used to form the relationship between the torques produced by the motor and the output torques measured

$$\frac{T_s(j\omega)}{T_o(j\omega)} = \frac{(5.85 \times 10^{-3}(-\omega^2) + 3.07(j\omega) + 8.1 \times 10^4)}{8.1 \times 10^4} \quad (32)$$

Figure 4 is a graph of the magnitude ratio of $T_s(j\omega)/T_o(j\omega)$ calculated from equation (32). This curve can be used to find the instantaneous value of torque by finding the magnitude ratio for a given frequency from figure 4 and multiplying by the magnitude of T_o at that frequency. The magnitude of T_o at the frequency of interest is the product of the constant C_T times the magnitude of the frequency component taken from the recorder.

Because of the problems associated with the calculation of C_T , the constant relating output voltage of the bridge to the torque's magnitude, the system is more valuable in relating the relative magnitude of the various frequency components than in measuring the absolute value of the components.

An interesting example of the response of the measuring system is displayed from the response to a series of impulses as shown in figure 5.

Other examples of the response of the system are shown in figures 6 and 7.

Figure 6 shows the effect of the instantaneous torque production of a single phase motor whenever the load is rapidly removed.

Figure 7 shows the effect on the instantaneous torque production of a capacitor split motor whenever the load is rapidly removed. As may be expected by comparing figure 6

to figure 7, the capacitor split motor operated more quietly than the same motor without the capacitor. Also, both motors operated more quietly while under load.

IV. CONCLUSIONS

The experimental results of this work agreed well with the predicted results. The main exception to the satisfactory results was the viscous-friction coefficient which was found to be small but was several orders of magnitude larger than the predicted value.

The major problems associated with the project were:

(1) difficult modeling of the motor-beam attachment; (2) difficulties in the selection of items affecting the viscous frequency coefficient; (3) binding within the system because of parts tolerance; (4) large instantaneous torque components at the motor's rotational angular velocity because of shaft warp, rotor imbalance, and mechanical misalignment; (5) handling of the small semiconductor strain gages; and (6) difficulty in obtaining a very stiff physical system without extensive modifications of the motor.

A digital computer was used as an aid in the calculations for the frequency compensation of the system. A computer program was written to solve the inverse of the transfer function for magnitude and phase at ten-Hertz increments. The computer's solution for magnitude is shown in figure 4⁽⁵⁾.

Several possible areas of additional work to reduce the data taken from the system are: (1) sampling the output so

(5) See Appendix D for the complete program and the tabulated solution of magnitude and phase for ten-Hertz frequency increments.

the data could be given to a digital computer along with a Fourier series program and the system's transfer function so that the magnitude and phase shift of component torques could be quickly calculated; (2) the simulation of the inverse of the transfer function on an analog computer so as to obtain direct recordings for the instantaneous torque developed; (3) other configurations of stator restraints and/or a motor with a specially designed frame could be used in an attempt to raise the natural frequency; and (4) the use of a calibrated load device in order to get an accurate dynamic calibration.

The system is presently being used to measure and record the instantaneous torque produced by a single phase motor. The measurements are made at different load conditions and different phase splitting of the start windings. From these recordings the magnitude of the different frequency components are taken and multiplied by the frequency's compensating factor taken from figure 4. This information should be useful in future research concerning the single phase motor.

APPENDIX A
DESCRIPTION OF EQUIPMENT

I. Motor

1/6 Horsepower	110 Volts	3.0 Amperes
1100/1050/950 RPM	60 Cycle/Second	Single Phase
50° C Rise	Frame 48Y	

Model K55HXBPB - 1216

Stator's weight - 5 pounds End Bells' weight - 1/2 Pound

Stator's diameter: inside - 1.6 inches, outside - 2.8 inches

Emerson Electric Co.

II. Brake

1.5 Horsepower at 1800 RPM

Excitation: 90 Volts

Dynamatic Division of Adjusto-Brake Inc.

III. Recorder

Model 447 - Oscillagraph

Century Electronics

IV. Pre-Amplifier

Model 530 CR

Century Electronics

V. Brake Excitation

Heathkit Variable Voltage Regulated Power Supply

Model PS-3

VI. Oscilloscope

Hewlett-Packard

Model 1402

VII. Strain Gage

Model SP5-35-500 Nominal Resistance 5000 ohms

Nominal gage factor 148 Active gage length - 0.35 inch

BLH Electronics

APPENDIX B

Methods of Data Reduction used with the Baldwin-Lima-Hamilton Strain Gage and Strain Sensitivity Tables.

The gage factor of a semi-conductor strain gage is a function of temperature and strain level. In order to determine the gage factor at room temperature for a bonded gage, the resistance before and after bonding or mounting must be known. Let R_B be the resistance of the gage after bonding and R_O be the unbonded resistance; in this case, $R_B = 5784$ and $R_O = 5900$. Then the unit resistance change in bonding

$$\frac{R_B - R_O}{R_O} = \frac{5784 - 5900}{5900} = -0.0200 \frac{\Omega}{\Omega} \quad (B1)$$

Using strain sensitivity tables, the value of the unit resistance change at 80°F. gives a pre-strain value of approximately $-125 \frac{\mu - \text{in.}}{\text{in.}}$

The equation used to calculate the gage factor of the gage in a constant-current circuit is;

$$\text{G.F.} = \text{G.F.}' + C_2'(2\epsilon + \epsilon_x)10^{-6} \quad (B2)$$

$$\frac{R_O}{R_B} = 156.3 + 71 \times 10^{-3} = 156.4$$

To determine the gage factor for a constant voltage circuit

$$\text{G.F.} = \frac{2 \Delta R}{(2R_B + R) \epsilon_x} \quad (B3)$$

where

$$R = R_B \epsilon_x \times G.F._{cc}$$

so

$$\begin{aligned} G.F. &= \frac{2 \times 5784 \times 50 \times 10^{-6} \times 156.4 \times 10^6}{(2 \times 5784 + 5784 \times 50 \times 10^{-6} \times 156.4)50} \\ &= \frac{9.04 \times 10^{-6}}{(11520 + 4.5)50} = 157 \end{aligned} \quad (B4)$$

This result indicates that the change of gage factor is small when the bonding resistance change is small and the expected strain level is small.

Other corrections which can be applied to the readings are linearity corrections and temperature corrections.

Since ϵ_x is small no linearity correction was made.

Two corrections are required for the temperature effects:

(1) Changes of resistance because of the temperature coefficient of the silicon material and

(2) Strain caused by the change of length of the steel beam with temperature.

The first correction is made by the use of figure 8. This is a curve provided by the manufacturer for the particular type gage. For a temperature of 85°F the change in R with respect to R_0 is found to be 2 percent.

Since the linear coefficient of expansion of steel is about 6.5 ppm/F°, then the apparent strain increase at a 10°F change would be 65 micro-in./in.

Since the apparent strain and the temperature coefficient changes were not large enough to appreciably affect

the gage constant, their effects were not required in the test. These effects can be neglected because the impulse and step response work were performed at constant temperature and the instantaneous torque measurements are made in such a short interval of time that the temperature is approximately constant. However, in some of the instantaneous torque measurements, the slight drift of the signal is attributed to the slow temperature change.

BLH SEMICONDUCTOR STRAIN GAGES

UNIT RESISTANCE CHANGE VERSUS STRAIN LEVEL AND TEMPERATURE

P-TYPE GF 156.3 C2 2,800 T-0 77F

R-0 IS FUNCTION OF T - USE ENCLOSED TEMPERATURE COEFFICIENT CURVE
ZERO STRAIN - UNSTRESSED CONDITION AT T-0

STRAIN U IN/IN	TEMPERATURE DEGREES F						
	0	20	40	60	80	100	120
-3000	-.5130	-.4930	-.4745	-.4573	-.4413	-.4264	-.4125
-2950	-.5050	-.4853	-.4670	-.4501	-.4344	-.4197	-.4059
-2900	-.4970	-.4776	-.4596	-.4429	-.4274	-.4129	-.3994
-2850	-.4889	-.4698	-.4521	-.4357	-.4204	-.4062	-.3929
-2800	-.4809	-.4621	-.4447	-.4285	-.4134	-.3994	-.3863
-2750	-.4728	-.4543	-.4372	-.4212	-.4064	-.3926	-.3797
-2700	-.4648	-.4465	-.4296	-.4140	-.3994	-.3859	-.3732
-2650	-.4566	-.4387	-.4221	-.4067	-.3924	-.3790	-.3666
-2600	-.4485	-.4309	-.4146	-.3994	-.3853	-.3722	-.3600
-2550	-.4404	-.4230	-.4070	-.3921	-.3783	-.3654	-.3533
-2500	-.4322	-.4152	-.3994	-.3848	-.3712	-.3586	-.3467
-2450	-.4241	-.4073	-.3918	-.3775	-.3641	-.3517	-.3401
-2400	-.4159	-.3994	-.3842	-.3701	-.3570	-.3448	-.3334
-2350	-.4076	-.3915	-.3766	-.3627	-.3499	-.3379	-.3267
-2300	-.3994	-.3836	-.3690	-.3554	-.3428	-.3311	-.3201
-2250	-.3911	-.3756	-.3613	-.3480	-.3356	-.3241	-.3134
-2200	-.3829	-.3677	-.3536	-.3406	-.3285	-.3172	-.3067
-2150	-.3746	-.3597	-.3459	-.3332	-.3213	-.3103	-.3000
-2100	-.3663	-.3517	-.3382	-.3257	-.3141	-.3033	-.2932
-2050	-.3579	-.3437	-.3305	-.3183	-.3069	-.2964	-.2865
-2000	-.3496	-.3356	-.3228	-.3108	-.2997	-.2894	-.2798
-1950	-.3412	-.3276	-.3150	-.3033	-.2925	-.2824	-.2730
-1900	-.3328	-.3195	-.3072	-.2958	-.2853	-.2754	-.2662
-1850	-.3244	-.3114	-.2994	-.2883	-.2780	-.2684	-.2594
-1800	-.3160	-.3033	-.2916	-.2808	-.2707	-.2614	-.2526
-1750	-.3075	-.2952	-.2838	-.2732	-.2635	-.2543	-.2458
-1700	-.2991	-.2871	-.2760	-.2657	-.2562	-.2473	-.2390
-1650	-.2906	-.2789	-.2681	-.2581	-.2489	-.2402	-.2322

U	IN/IN	0	20	40	60	80	100	120
-1600	-.2821	-.2707	-.2603	-.2505	-.2415	-.2332	-.2253	-.2185
-1550	-.2736	-.2626	-.2524	-.2429	-.2342	-.2261	-.2185	-.2116
-1500	-.2650	-.2543	-.2445	-.2353	-.2269	-.2190	-.2116	-.2047
-1450	-.2565	-.2461	-.2366	-.2277	-.2195	-.2119	-.2047	-.1978
-1400	-.2479	-.2379	-.2286	-.2201	-.2121	-.2047	-.1976	-.1909
-1350	-.2393	-.2296	-.2207	-.2124	-.2047	-.1976	-.1904	-.1840
-1300	-.2307	-.2213	-.2127	-.2047	-.1973	-.1904	-.1833	-.1771
-1250	-.2220	-.2130	-.2047	-.1970	-.1899	-.1833	-.1761	-.1701
-1200	-.2134	-.2047	-.1967	-.1893	-.1825	-.1761	-.1689	-.1632
-1150	-.2047	-.1964	-.1887	-.1816	-.1750	-.1689	-.1617	-.1562
-1100	-.1960	-.1881	-.1807	-.1739	-.1676	-.1617	-.1545	-.1492
-1050	-.1873	-.1797	-.1726	-.1661	-.1601	-.1545	-.1473	-.1423
-1000	-.1786	-.1713	-.1646	-.1584	-.1526	-.1473	-.1423	-.1353
- 950	-.1698	-.1629	-.1565	-.1506	-.1451	-.1400	-.1353	-.1282
- 900	-.1611	-.1545	-.1484	-.1428	-.1376	-.1328	-.1282	-.1212
- 850	-.1523	-.1460	-.1403	-.1350	-.1301	-.1255	-.1212	-.1142
- 800	-.1435	-.1376	-.1322	-.1272	-.1225	-.1182	-.1142	-.1071
- 750	-.1346	-.1291	-.1240	-.1193	-.1150	-.1109	-.1071	-.1001
- 700	-.1258	-.1206	-.1159	-.1115	-.1074	-.1036	-.1001	-.0930
- 650	-.1169	-.1121	-.1077	-.1036	-.0998	-.0963	-.0930	-.0859
- 600	-.1080	-.1036	-.0995	-.0957	-.0922	-.0890	-.0859	-.0788
- 550	-.0991	-.0951	-.0913	-.0878	-.0846	-.0816	-.0788	-.0717
- 500	-.0902	-.0865	-.0831	-.0799	-.0770	-.0742	-.0717	-.0646
- 450	-.0813	-.0779	-.0748	-.0720	-.0693	-.0669	-.0646	-.0575
- 400	-.0723	-.0693	-.0666	-.0640	-.0617	-.0595	-.0575	-.0503
- 350	-.0633	-.0607	-.0583	-.0561	-.0540	-.0521	-.0503	-.0432
- 300	-.0543	-.0521	-.0500	-.0481	-.0463	-.0447	-.0432	-.0360
- 250	-.0453	-.0434	-.0417	-.0401	-.0386	-.0373	-.0360	-.0288
- 200	-.0363	-.0348	-.0334	-.0321	-.0309	-.0298	-.0288	-.0216
- 150	-.0272	-.0261	-.0251	-.0241	-.0232	-.0224	-.0216	-.0144
- 100	-.0182	-.0174	-.0167	-.0161	-.0155	-.0149	-.0144	-.0072
- 50	-.0091	-.0087	-.0083	-.0080	-.0077	-.0074	-.0072	-.0000
0	-.0000	-.0000	-.0000	-.0000	-.0000	-.0000	-.0000	-.0000
50	.0091	.0087	.0083	.0080	.0077	.0074	.0072	.0144
100	.0182	.0175	.0168	.0161	.0155	.0150	.0144	.0216
150	.0274	.0262	.0252	.0242	.0233	.0225	.0217	.0290
200	.0366	.0351	.0336	.0323	.0311	.0300	.0290	.0363
250	.0458	.0439	.0421	.0405	.0390	.0376	.0363	.0436
300	.0550	.0527	.0506	.0486	.0468	.0451	.0436	.0509
350	.0643	.0616	.0591	.0568	.0547	.0527	.0509	

U IN/IN	0	20	40	60	80	100	120
400	.0735	.0705	.0676	.0650	.0626	.0603	.0582
450	.0828	.0793	.0761	.0732	.0704	.0679	.0655
500	.0921	.0882	.0847	.0814	.0784	.0755	.0729
550	.1014	.0972	.0932	.0896	.0863	.0831	.0803
600	.1108	.1061	.1018	.0979	.0942	.0908	.0876
650	.1201	.1151	.1104	.1061	.1021	.0984	.0950
700	.1295	.1241	.1190	.1144	.1101	.1061	.1024
750	.1389	.1331	.1277	.1227	.1181	.1138	.1098
800	.1483	.1421	.1363	.1310	.1261	.1215	.1172
850	.1578	.1511	.1450	.1393	.1341	.1292	.1247
900	.1672	.1601	.1536	.1476	.1421	.1369	.1321
950	.1767	.1692	.1623	.1560	.1501	.1446	.1396
1000	.1862	.1783	.1710	.1643	.1581	.1524	.1470
1050	.1957	.1874	.1798	.1727	.1662	.1601	.1545
1100	.2053	.1965	.1885	.1811	.1743	.1679	.1620
1150	.2148	.2057	.1973	.1895	.1823	.1757	.1695
1200	.2244	.2148	.2060	.1979	.1904	.1835	.1770
1250	.2340	.2240	.2148	.2063	.1985	.1913	.1846
1300	.2436	.2332	.2236	.2149	.2067	.1991	.1921
1350	.2532	.2424	.2324	.2233	.2148	.2070	.1997
1400	.2628	.2516	.2413	.2318	.2230	.2148	.2072
1450	.2725	.2608	.2501	.2402	.2311	.2227	.2148
1500	.2822	.2701	.2590	.2488	.2393	.2306	.2224
1550	.2919	.2794	.2679	.2573	.2475	.2384	.2300
1600	.3016	.2887	.2768	.2658	.2557	.2463	.2376
1650	.3114	.2980	.2857	.2744	.2639	.2542	.2452
1700	.3211	.3073	.2947	.2829	.2722	.2622	.2529
1750	.3309	.3167	.3036	.2915	.2804	.2701	.2605
1800	.3407	.3260	.3126	.3001	.2887	.2781	.2682
1850	.3505	.3354	.3215	.3087	.2970	.2860	.2759
1900	.3604	.3448	.3305	.3174	.3052	.2940	.2835
1950	.3702	.3542	.3396	.3260	.3135	.3020	.2912
2000	.3801	.3637	.3486	.3347	.3219	.3100	.2989
2050	.3900	.3731	.3576	.3433	.3302	.3180	.3067
2100	.3999	.3826	.3667	.3520	.3385	.3260	.3144
2150	.4098	.3921	.3758	.3607	.3469	.3341	.3221
2200	.4198	.4016	.3849	.3695	.3553	.3421	.3299
2250	.4298	.4111	.3940	.3782	.3637	.3502	.3377
2300	.4398	.4206	.4031	.3869	.3721	.3583	.3455
2350	.4498	.4302	.4123	.3957	.3805	.3664	.3532

U IN/IN	0	20	40	60	80	100	120
2400	.4598	.4398	.4214	.4045	.3889	.3745	.3611
2450	.4698	.4494	.4306	.4133	.3973	.3826	.3689
2500	.4799	.4590	.4398	.4221	.4058	.3907	.3767
2550	.4900	.4686	.4490	.4309	.4143	.3989	.3845
2600	.5001	.4782	.4582	.4398	.4228	.4070	.3924
2650	.5102	.4879	.4675	.4486	.4313	.4152	.4003
2700	.5204	.4976	.4767	.4575	.4398	.4234	.4061
2750	.5305	.5073	.4860	.4664	.4483	.4316	.4160
2800	.5407	.5170	.4953	.4753	.4568	.4398	.4239
2850	.5509	.5267	.5046	.4842	.4654	.4480	.4318
2900	.5611	.5365	.5139	.4931	.4740	.4562	.4398
2950	.5714	.5463	.5232	.5020	.4825	.4645	.4477
3000	.5816	.5560	.5326	.5110	.4911	.4727	.4556

APPENDIX C

METHODS AND PROCEDURES USED IN THE EXPERIMENTAL DETERMINATION
OF THE CONSTANTS:I. Mass Moment of Inertia of the Stator and Beam

The experimental procedure for finding J_s required a test setup which permitted the stator to be free to rotate about its center of gravity. This was accomplished by using the motor shaft to suspend the motor vertically, Then a small, lightweight line was wrapped around the stator and over a low inertia pulley to a weight tray. By means of changing the amount of weight, the friction between the stator and the rotor could be determined; then by slightly increasing the weight, the mass moment of inertia could be determined.

The motion of the stator when it is free to rotate about center of gravity is described by

$$T = J_s \ddot{\theta} + f_s \dot{\theta} + C \quad (C1)$$

If a constant torque, T_1 , is applied so that the system rotates at a constant, very low angular velocity, then

$$\dot{\theta} = 0$$

and

$$f_s \dot{\theta} \approx 0$$

so equation (C1) reduces to

$$T_1 \approx C \quad (C2)$$

Now by increasing the torque applied to the stator to a new value, T_2 so that the system is subjected to a constant acceleration, then equation (C1) becomes

$$T_2 \cong J_s \ddot{\theta} + c \quad (C3)$$

and by substituting equation (C2) into equation (C3)

$$T_2 = J_s \ddot{\theta} + T_1 \quad (C4)$$

or rearranging

$$J_s = \frac{T_2 - T_1}{\ddot{\theta}} \quad (C5)$$

For this system, T_1 was found to be 0.0309 ft - lbs. and for a T_2 of 0.0360 ft - lbs., $\ddot{\theta}$ was found to be 0.88 rad/sec.², so substituting these values into equation (C5) gives

$$J_s = 5.85 \times 10^{-3} \text{ slug - ft.}^2 \quad (C6)$$

II. Damped Natural Frequency ω_d , Natural Frequency ω_n , and Damping Factor ζ .

The impulse response shown in figure 5 indicates that the output takes approximately 1.7 milliseconds for one cycle, therefore

$$\omega_d = \frac{2\pi}{1.7 \times 10^{-3}} = 3700 \text{ radians/second} \quad (C7)$$

Also from figure 5, the damping is found to reduce the waveform from approximately 2 units to 0.5 units in 5.3×10^{-3} seconds, therefore

$$0.5 = 2.0e^{-\sigma} (0.0053) \quad (C8)$$

and solving equation (C8) for

$$\sigma = 262 \quad (C9)$$

Now

$$\omega_d = \sqrt{(1 - \zeta^2)} \omega_n \quad (C10)$$

and

$$\zeta \omega_n = \sigma \quad (C11)$$

so by substituting ω_n from equation (C11) into equation (C10) gives

$$\omega_d^2 = (1 - \zeta^2) \frac{\sigma^2}{\zeta^2} \quad (C12)$$

Putting in values for ω_d and σ from equations (C7) and (C9) and solving for ζ yields

$$\zeta = 0.0705 \quad (C13)$$

From equation (C11)

$$\zeta \omega_n = \sigma$$

so substituting the values of σ and ζ into equation (C11) gives

$$\omega_n = \frac{262}{0.0705} = 3720 \text{ rad./sec.} \quad (C14)$$

and

$$f_n = 592 \text{ Hertz}$$

III. Viscous Friction Coefficient, f_s , and Torsional-Spring Constant K_T

f_s is determined by solving the characteristic equation taken from equation (20), the transfer function of the measuring system. The characteristic equation is

$$s^2 J_s + s f_s + K_T = 0 \quad (C15)$$

Solving for s gives

$$s = \frac{f_s}{2J_s} \pm \frac{\sqrt{f_s^2 - 4J_s K_T}}{2J_s} \quad (C16)$$

and since $s = \sigma + j\omega_d$

$$\sigma = -\frac{f_s}{2J_s} \quad (C17)$$

therefore, substituting the values of σ and J_S into equation (C17) and rearranging

$$\begin{aligned} f_S &= 2(262)(5.85 \times 10^{-3}) \\ &= 3.07 \frac{\text{ft.} - \text{lbs.}}{\text{rad./sec.}} \end{aligned} \quad (\text{C18})$$

Also

$$\omega_d = \sqrt{\frac{4J_S K_T - f_S^2}{2J_S}} \quad (\text{C19})$$

so rearranging and solving for K_T gives

$$K_T = \frac{4J_S^2 \omega_d^2 + f_S^2}{4J_S} \quad (\text{C20})$$

then substituting values from equations (C6), (C7) and (C18) yields

$$K_T = \frac{1875.0 + 9.4}{23.4 \times 10^{-3}} = 8.1 \times 10^4 \frac{\text{ft.} - \text{lbs.}}{\text{rad.}} \quad (\text{C21})$$

IV. Torque-to-Voltage Conversion Factor, C_T

The deflection of the recorder for a fifteen pound test load was 12.0 divisions. The recorder's sensitivity was 238×10^{-6} volts/division, therefore

$$E_o = (238 \times 10^{-6})(12) = 2.86 \times 10^{-3} \text{ volts} \quad (\text{C22})$$

so by defining the relationship

$$r_m(F_{\text{applied}}) = C_T(E_o) \quad (\text{C23})$$

where

F_{applied} is the test force in pounds

and

C_T is the torque conversion constant in ft. - lbs./volt

Then

$$\frac{2.8 \times 15}{12} = (2.86 \times 10^{-3}) C_T \quad (C24)$$

and

$$C_T = 1.23 \times 10^3 \text{ ft. - lbs./volt} \quad (C25)$$

APPENDIX D

Computer Program For Inverse Transfer Function And
Tables of Magnitude And Phase For Ten-Hertz Increments

```

C      MAG. AND PHASE PLOT OF G AS A FUNC. OF F
      DIMENSION G(300),ANG(300),F(300)
      A=C.00585
      A=A*((2.C*3.14159265)**2)
      P=3.07
      R=R*(2.C*3.14159265)
      C=81000.0
      F(1)=0.C
      DF=10.0
      WRITE(3,100)
      DO 30 J=1,251
      REAL=C-A*(F(J)**2)
      AMAG=R*F(J)
      ARG=AMAG/REAL
      G(J)=SQRT(REAL**2+AMAG**2)
      G(J)=G(J)/C
      ANG(J)=ATAN(ARG)
      IF(ARC)10,20,20
10     ANG(J)=ANG(J)+3.14159265
20     ANG(J)=ANG(J)*(180.0/3.14159265)
      WRITE(3,200)F(J),G(J),ANG(J)
30     F(J+1)=F(J)+DF
100    FORMAT(4X,9HFREQUENCY,9X,9HMAGNITUDE,11X,5HANGLE)
200    FORMAT(4F18.8)
C      PLOT OF MAGNITUDE G VS FREQUENCY
      CALL PENPOS('HERTEL, THOMAS',14,C)
      CALL NEWPLT(2.5,3.5,8.0)
      CALL ORIGIN(0.0,0.0)
      CALL XSCALE(0.0,2500.0,5.0)
      CALL YSCALE(0.0,20.0,6.0)
      CALL XAXIS(100.0)
      CALL YAXIS(1.0)
      CALL XYPLT(F,G,250,1,-1)
      CALL PEN(2)
      CALL SYM(.75,-1.00,0.21,'FREQUENCY IN HERTZ',0.0,18)
      CALL SYM(-0.80,1.5,0.21,'MAGNITUDE RATIO',90.0,15)
      XPIN=C.80
      RN=500.0
      DO 40 J=1,5
      CALL NUM(XBIN,-0.30,0.14,RN,0.0,-1)
      XBIN=XBIN+1.0
40     RN=RN+500.0
      YBIN=-0.07
      RN=0.0
      DO 50 J=1,5
      CALL NUM(-0.40,YBIN,0.14,RN,C.0,-1)
      YBIN=YBIN+1.5
50     RN=RN+5.0
      CALL ENDPLT
      CALL LSTPLT
      CALL EXIT
      STOP
      END

```

FREQUENCY	MAGNITUDE	ANGLE
0.C	0.99999923	0.0
10.00000000	0.99971682	0.13648307
20.00000000	0.99886960	0.27319813
30.00000000	0.99745828	0.41037905
40.00000000	0.99548221	0.54826206
50.00000000	0.99294287	0.68708646
60.00000000	0.98983794	0.82709914
70.00000000	0.98616898	0.96855152
80.00000000	0.98193592	1.11170483
90.00000000	0.97713888	1.25682831
100.00000000	0.97177851	1.40420723
110.00000000	0.96585488	1.55413723
120.00000000	0.95936728	1.70693016
130.00000000	0.95231634	1.86291695
140.00000000	0.94470370	2.02245045
150.00000000	0.93652773	2.18590355
160.00000000	0.92779088	2.35367956
170.00000000	0.91849148	2.52621078
180.00000000	0.90863115	2.70396614
190.00000000	0.89821064	2.88745022
200.00000000	0.88722914	3.07721710
210.00000000	0.87568903	3.27386570
220.00000000	0.86359024	3.47805595
230.00000000	0.85093439	3.69051170
240.00000000	0.83772063	3.91204834
250.00000000	0.82395136	4.14354038
260.00000000	0.80962807	4.38598156
270.00000000	0.79475141	4.64047813
280.00000000	0.77932233	4.90825844
290.00000000	0.76334298	5.19072151
300.00000000	0.74681538	5.48943615
310.00000000	0.72974175	5.80619335
320.00000000	0.71212441	6.14301682
330.00000000	0.69396633	6.50224400
340.00000000	0.67527097	6.88655853
350.00000000	0.65604210	7.29906082
360.00000000	0.63628411	7.74336433
370.00000000	0.61600256	8.22369099
380.00000000	0.59520358	8.74501896
390.00000000	0.57389468	9.31326294

400.C0000000	0.55208492	9.93546295
410.C0000000	0.52978516	10.62011719
420.C0000000	0.50700849	11.37751007
430.C0000000	0.48377162	12.22028065
440.C0000000	0.46009451	13.16402149
450.C0000000	0.43600303	14.22824287
460.C0000000	0.41152990	15.43757629
470.C0000000	0.38671720	16.82356262
480.C0000000	0.36162084	18.42704773
490.C0000000	0.33631480	20.30165100
500.C0000000	0.31090021	22.51869202
510.C0000000	0.28551728	25.17430115
520.C0000000	0.26036435	28.39930725
530.C0000000	0.23572874	32.37251282
540.C0000000	0.21203291	37.33609009
550.C0000000	0.18990296	43.60678101
560.C0000000	0.17026615	51.55773926
570.C0000000	0.15442836	61.51988220
580.C0000000	0.14403582	73.52375793
590.C0000000	0.14070231	86.94786072
600.C0000000	0.14530951	100.48306274
610.C0000000	0.15752918	112.75756836
620.C0000000	0.17611670	123.03399658
630.C0000000	0.19959891	131.26655579
640.C0000000	0.22672671	137.76152039
650.C0000000	0.25658786	142.89569092
660.C0000000	0.28855205	146.99621582
670.C0000000	0.32219207	150.31611633
680.C0000000	0.35721606	153.04267883
690.C0000000	0.39342195	155.31297302
700.C0000000	0.43066669	157.22766113
710.C0000000	0.468884745	158.86117554
720.C0000000	0.50788850	160.26950073
730.C0000000	0.54773313	161.49511719
740.C0000000	0.58833843	162.57073975
750.C0000000	0.62967104	163.52188110
760.C0000000	0.67170483	164.36882019
770.C0000000	0.71441996	165.12757874
780.C0000000	0.75779831	165.81118774
790.C0000000	0.80182713	166.43028259
800.C0000000	0.84649456	166.99357605
810.C0000000	0.89179397	167.50825500
820.C0000000	0.93771523	167.98040771
830.C0000000	0.98425382	168.41513062
840.C0000000	1.03140163	168.81675720
850.C0000000	1.07915783	169.18885803
860.C0000000	1.12751484	169.53474426
870.C0000000	1.17647171	169.85700989
880.C0000000	1.22602463	170.15814209
890.C0000000	1.27617073	170.44004822
900.C0000000	1.32690907	170.70466614
910.C0000000	1.37823486	170.95350647
920.C0000000	1.43015003	171.18797302
930.C0000000	1.48265076	171.40927124
940.C0000000	1.53573608	171.61854553
950.C0000000	1.58940601	171.81678772
960.C0000000	1.64365768	172.00486755
970.C0000000	1.69849110	172.18348694
980.C0000000	1.75390339	172.35342407
990.C0000000	1.80989742	172.51531982

1000.000000000	1.86647129	172.66969299
1010.000000000	1.92362213	172.81716919
1020.000000000	1.98135090	172.95808411
1030.000000000	2.03965759	173.09300232
1040.000000000	2.09854126	173.22222900
1050.000000000	2.15800095	173.34614563
1060.000000000	2.21803856	173.46516418
1070.000000000	2.27865028	173.57942200
1080.000000000	2.33983707	173.68934631
1090.000000000	2.40159988	173.79513550
1100.000000000	2.46393585	173.89698792
1110.000000000	2.52684784	173.99523926
1120.000000000	2.59033394	174.08998108
1130.000000000	2.65439415	174.18139648
1140.000000000	2.71902847	174.26976013
1150.000000000	2.78423500	174.35516357
1160.000000000	2.85001659	174.43772888
1170.000000000	2.91637039	174.51766968
1180.000000000	2.98329735	174.59509277
1190.000000000	3.05079842	174.67012024
1200.000000000	3.11887169	174.74284363
1210.000000000	3.18751812	174.81338501
1220.000000000	3.25673389	174.88185120
1230.000000000	3.32652473	174.94834900
1240.000000000	3.39688873	175.01293945
1250.000000000	3.46782589	175.07566833
1260.000000000	3.53933239	175.13670349
1270.000000000	3.61141205	175.19609070
1280.000000000	3.68406391	175.25390625
1290.000000000	3.75728798	175.31013489
1300.000000000	3.83108330	175.36492920
1310.000000000	3.90545273	175.41838074
1320.000000000	3.98039150	175.47039795
1330.000000000	4.05590153	175.52114868
1340.000000000	4.13198376	175.57066345
1350.000000000	4.20863914	175.61901855
1360.000000000	4.28586483	175.66616821
1370.000000000	4.36366177	175.71218872
1380.000000000	4.44202995	175.75720215
1390.000000000	4.52096939	175.80113220
1400.000000000	4.60048008	175.84408559
1410.000000000	4.68056393	175.88610840
1420.000000000	4.76121712	175.92720032
1430.000000000	4.84244061	175.96736145
1440.000000000	4.92423725	176.00669861
1450.000000000	5.00660419	176.04516602
1460.000000000	5.08954334	176.08280945
1470.000000000	5.17305279	176.11975098
1480.000000000	5.25713253	176.15586853
1490.000000000	5.34178352	176.19128418
1500.000000000	5.42700672	176.22598267
1510.000000000	5.51280022	176.26002502
1520.000000000	5.59916496	176.29335022
1530.000000000	5.68609905	176.32601929
1540.000000000	5.77360439	176.35809326
1550.000000000	5.86168194	176.38957214
1560.000000000	5.95032978	176.42050171
1570.000000000	6.03954792	176.45077515
1580.000000000	6.12933731	176.48054504
1590.000000000	6.21969795	176.50973511

1600.00000000	6.31062794	176.53842163
1610.00000000	6.40212917	176.56660461
1620.00000000	6.49420357	176.59431458
1630.00000000	6.58684635	176.62152100
1640.00000000	6.68005943	176.64823914
1650.00000000	6.77384377	176.67453003
1660.00000000	6.86819839	176.70037842
1670.00000000	6.96312523	176.72578430
1680.00000000	7.05862331	176.75074768
1690.00000000	7.15468884	176.77534485
1700.00000000	7.25132656	176.79949951
1710.00000000	7.34853554	176.82325745
1720.00000000	7.44631481	176.84671021
1730.00000000	7.54466438	176.86970520
1740.00000000	7.64358521	176.89237976
1750.00000000	7.74307537	176.91473389
1760.00000000	7.84313679	176.93669128
1770.00000000	7.94376850	176.95834351
1780.00000000	8.04497147	176.97964478
1790.00000000	8.14674377	177.00062561
1800.00000000	8.24908829	177.02133179
1810.00000000	8.35200214	177.04171753
1820.00000000	8.45548725	177.06176758
1830.00000000	8.55954266	177.08155823
1840.00000000	8.66416836	177.10105896
1850.00000000	8.76936436	177.12030029
1860.00000000	8.87513065	177.13925171
1870.00000000	8.98146820	177.15794373
1880.00000000	9.08837700	177.17636108
1890.00000000	9.19585419	177.19454956
1900.00000000	9.30390263	177.21247864
1910.00000000	9.41252232	177.23011780
1920.00000000	9.52171230	177.24760437
1930.00000000	9.63147163	177.26477051
1940.00000000	9.74180317	177.28175354
1950.00000000	9.85270309	177.29853382
1960.00000000	9.96417427	177.31503296
1970.00000000	10.07621670	177.33137512
1980.00000000	10.18882847	177.34748840
1990.00000000	10.30201149	177.36338306
2000.00000000	10.41576481	177.37907410
2010.00000000	10.53008842	177.39459229
2020.00000000	10.64458138	177.40989685
2030.00000000	10.76044750	177.42503357
2040.00000000	10.87648010	177.43994141
2050.00000000	10.99308586	177.45469666
2060.00000000	11.11026192	177.46928406
2070.00000000	11.22800732	177.48365784
2080.00000000	11.34632397	177.49786377
2090.00000000	11.46521091	177.51191711
2100.00000000	11.58466816	177.52578735
2110.00000000	11.70469570	177.53956604
2120.00000000	11.82529354	177.55311584
2130.00000000	11.94646168	177.56649780
2140.00000000	12.06819630	177.57972717
2150.00000000	12.19050980	177.59283447
2160.00000000	12.313337643	177.60578918
2170.00000000	12.436632575	177.61857605
2180.00000000	12.56085491	177.63124084
2190.00000000	12.68544006	177.64375305

2200.00000000	12.81060600	177.65611267
2210.00000000	12.93633842	177.66835022
2220.00000000	13.06262875	177.68048096
2230.00000000	13.18949318	177.69244385
2240.00000000	13.31693745	177.70425415
2250.00000000	13.44495010	177.71600342
2260.00000000	13.57354259	177.72758484
2270.00000000	13.70269108	177.73905945
2280.00000000	13.83240700	177.75036621
2290.00000000	13.96270275	177.76162720
2300.00000000	14.09356785	177.77272034
2310.00000000	14.22499943	177.78369141
2320.00000000	14.35699940	177.79457092
2330.00000000	14.48959255	177.80532837
2340.00000000	14.62272835	177.81599426
2350.00000000	14.75644398	177.82653309
2360.00000000	14.89072800	177.83697510
2370.00000000	15.02559185	177.84730530
2380.00000000	15.16101170	177.85751343
2390.00000000	15.29701233	177.86767578
2400.00000000	15.43357944	177.87768555
2410.00000000	15.57071590	177.88761902
2420.00000000	15.70843124	177.89746094
2430.00000000	15.84670353	177.90718079
2440.00000000	15.98555470	177.91685486
2450.00000000	16.12496948	177.92642212
2460.00000000	16.26495361	177.93586731
2470.00000000	16.40551758	177.94522095
2480.00000000	16.54664612	177.95451355
2490.00000000	16.68835449	177.96368408
2500.00000000	16.83061218	177.97280884

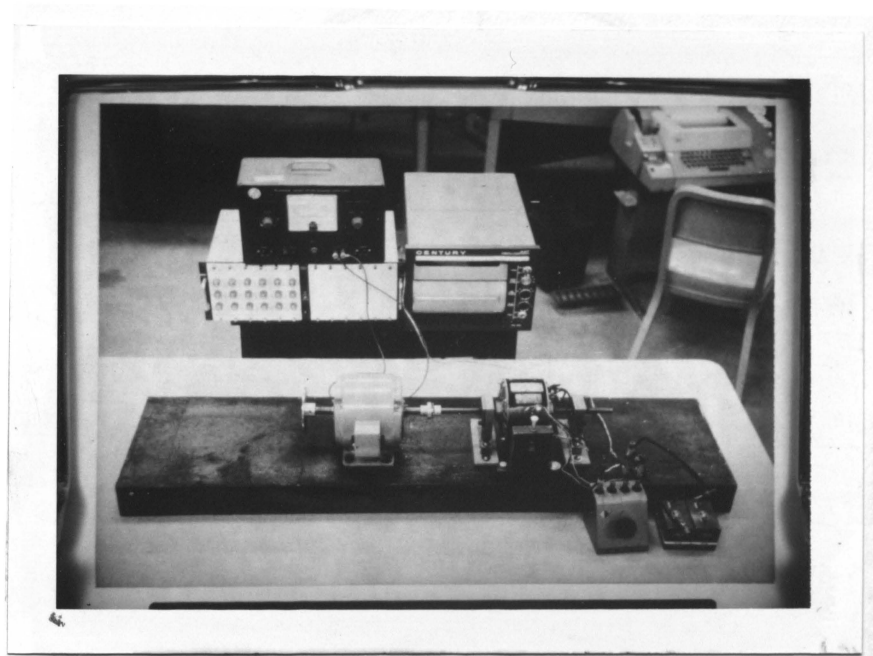


Figure 1. The Complete Test System

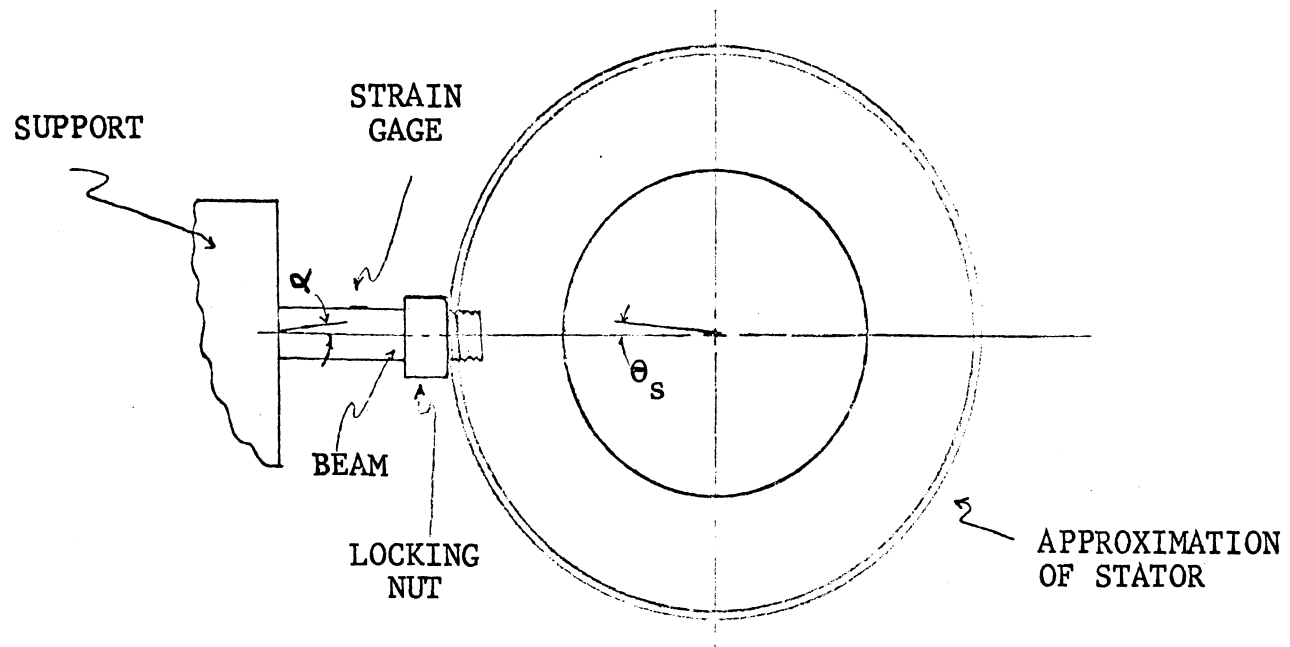


Figure 2. Drawing of Measuring Elements

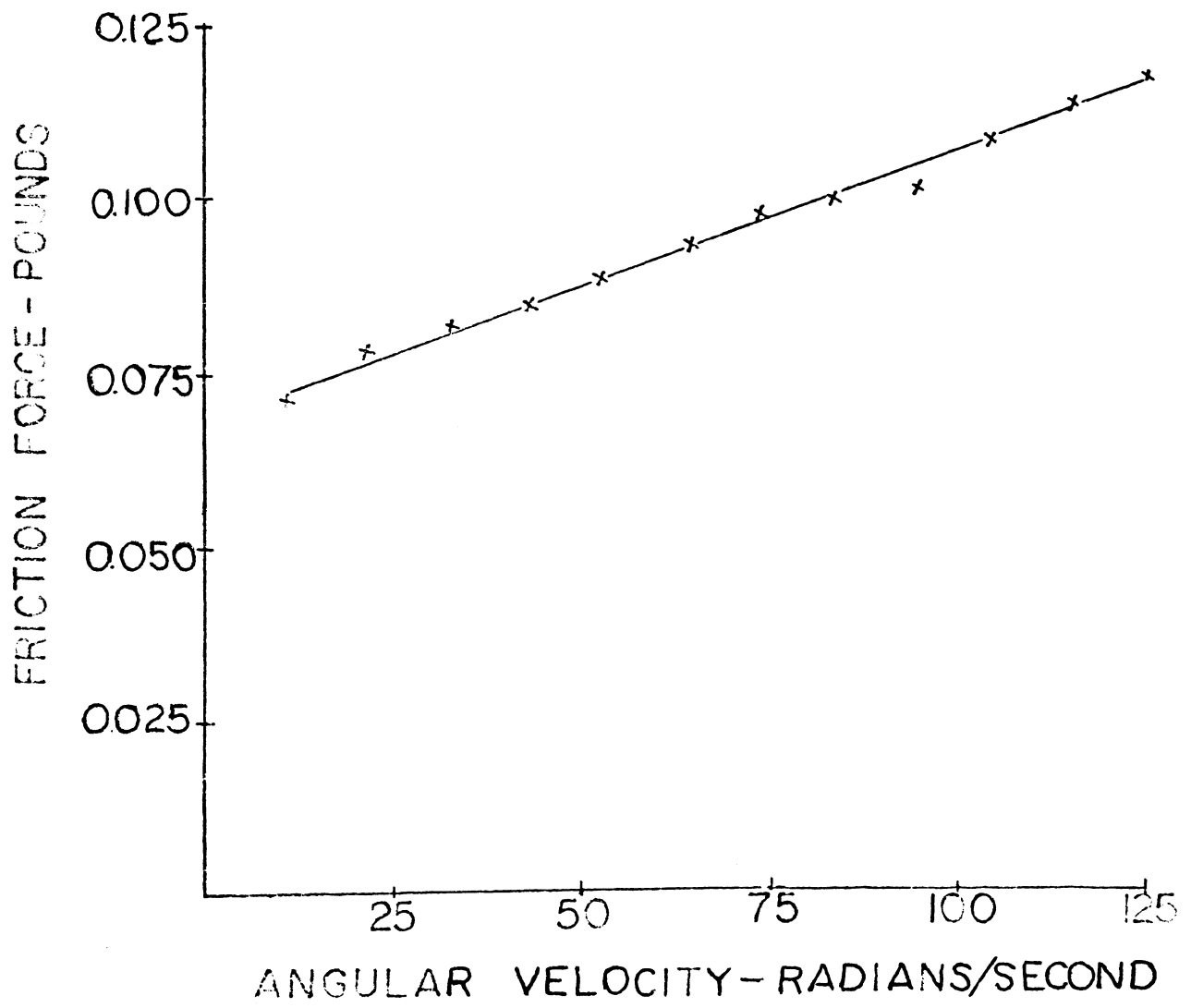


FIGURE 3. FRICTION FORCE vs ANGULAR VELOCITY

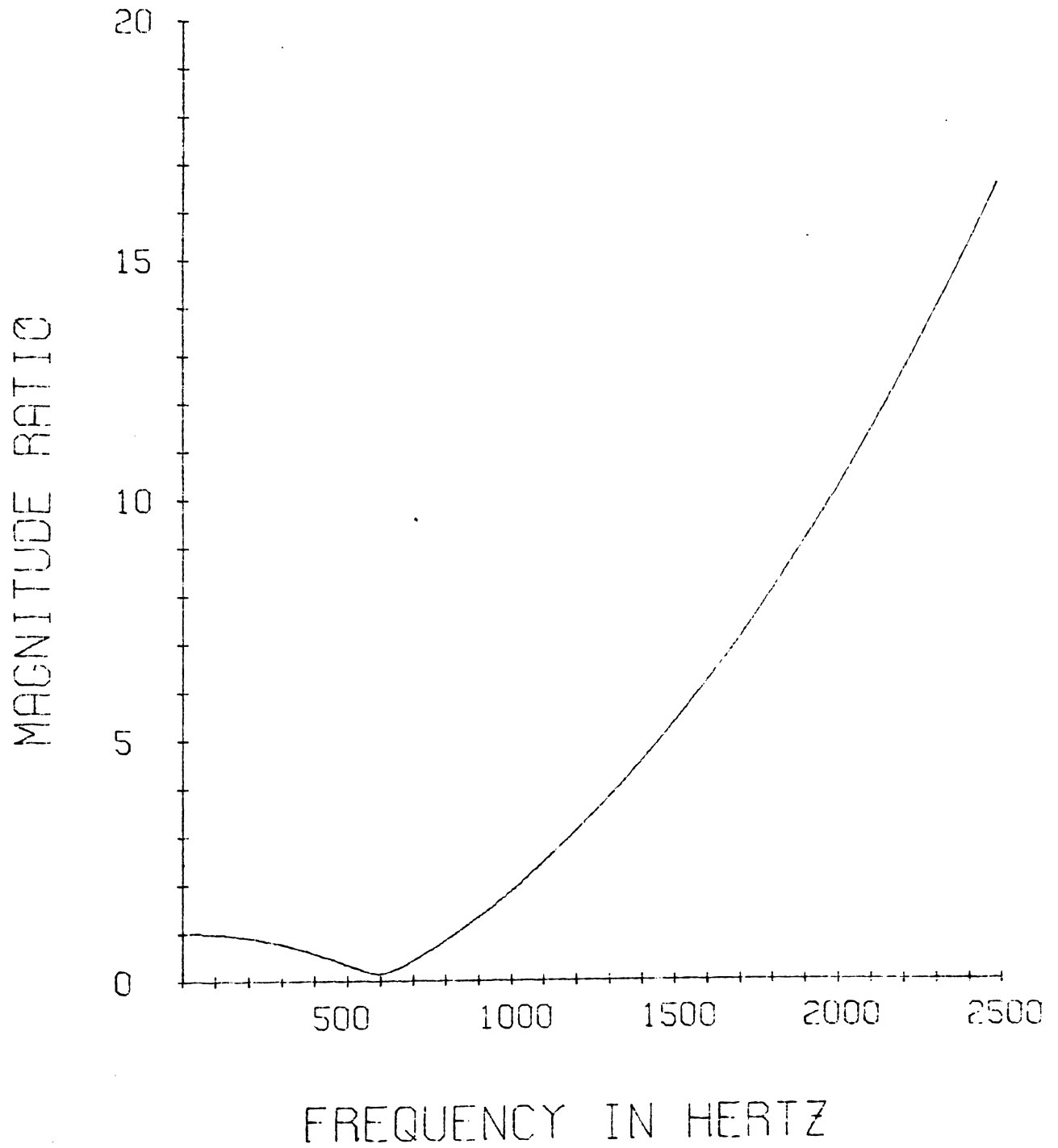


Figure 4. Plot of Inverse Transfer Function vs. Frequency

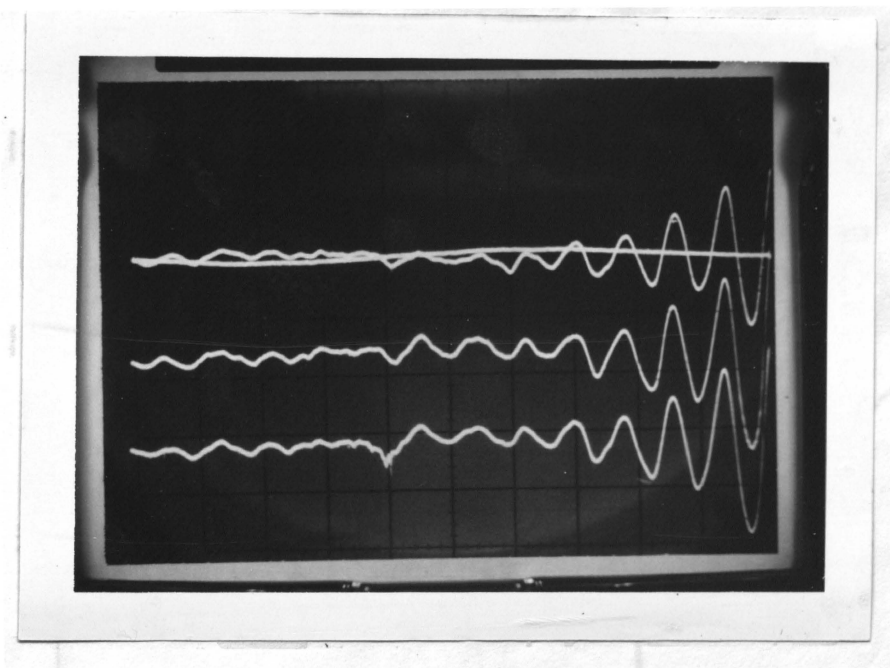


Figure 5. Responses to a Series of Impulses Loads

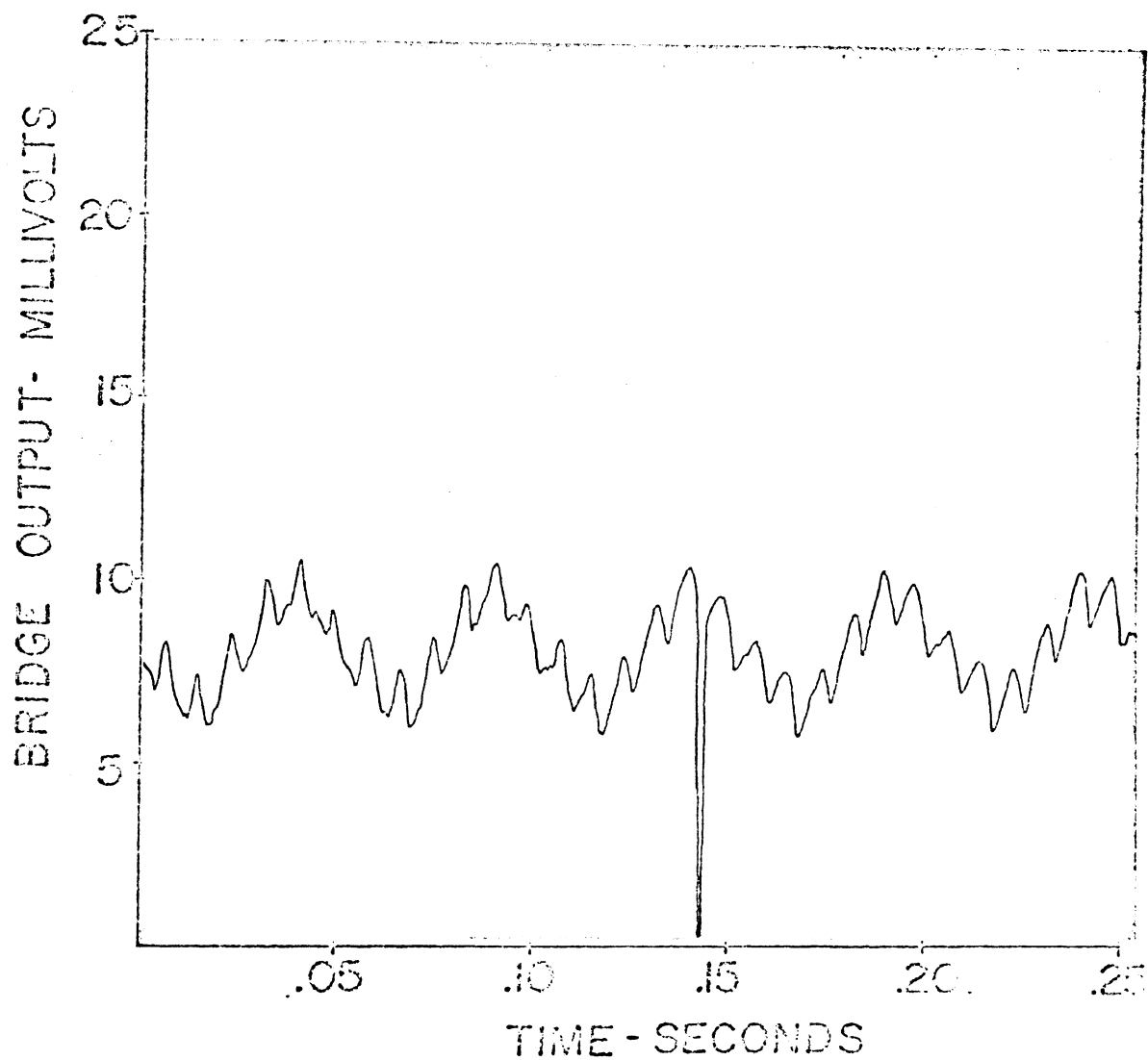


Figure 6: Response of a Single Phase Motor to a Load Change. The "Spike" was caused by capacitive coupling within the recorder when the load was removed.

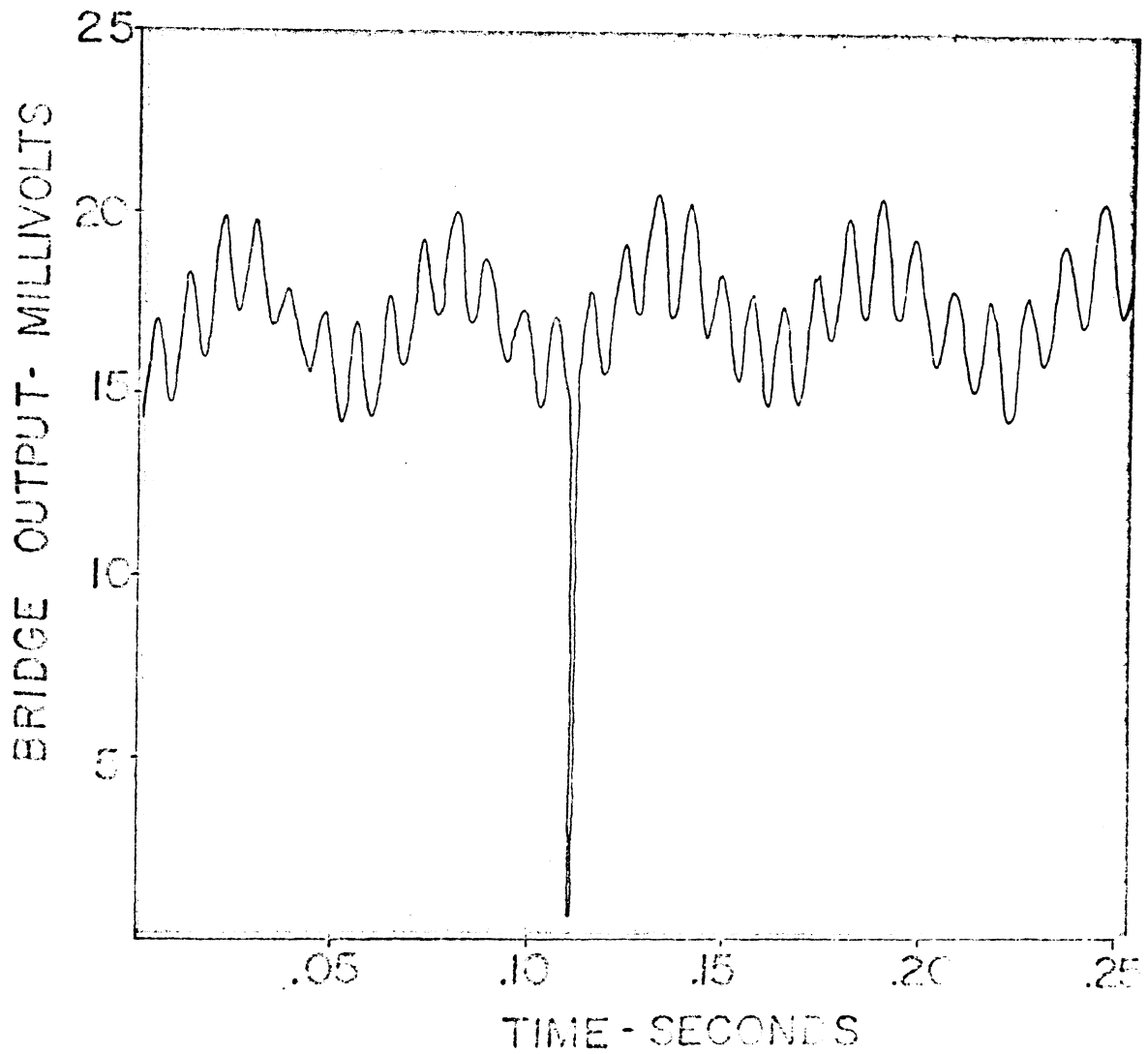


Figure 7. Response of a Capacitor Split Motor to a Load Change. The "spike" was primarily caused by capacitive coupling within the recorder when the load was removed.

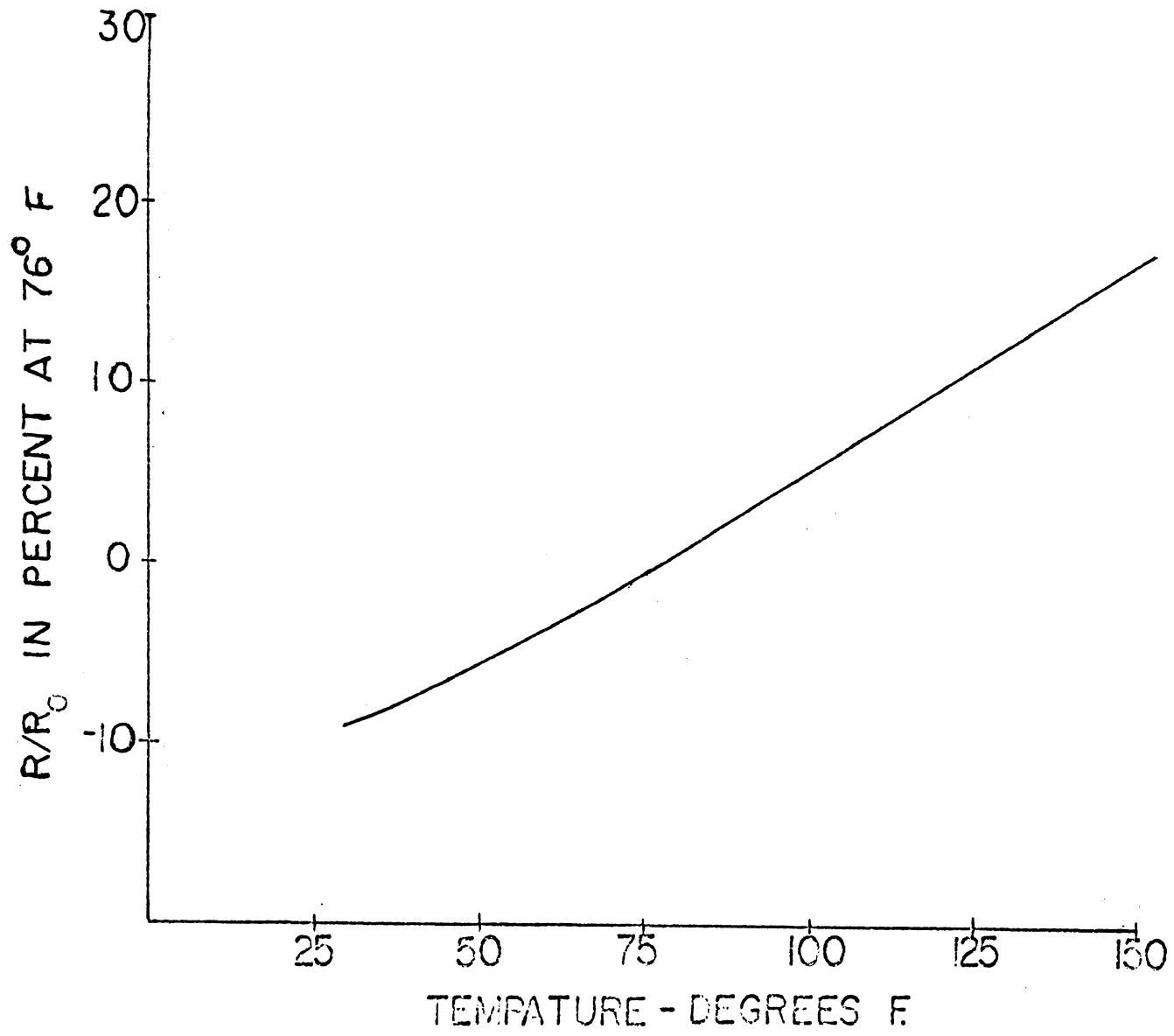


Figure 8. Temperature Coefficient of P-Type Silicon for Strain Gage

BIBLIOGRAPHY

- Higdon, Archie; Edward H. Ohlsen and William B. Stiles (1960) Mechanics of Materials. New York, The John Wiley and Sons, Inc. p. 502.
- D'Azzo, John J. and Constanting H. Houppis (1960) Feedback Control System Analysis and Synthesis. New York, Mc Graw-Hill Book Company, Inc. p.580.
- Thaler, George J. and Robert G. Brown (1960) Analysis and Design of Feedback Control Systems. New York Mc Graw-Hill Book Company, Inc. p. 648.
- Dorsey, James (1963) Semiconductor Strain Gage Handbook. Baldwin-Lima-Hamilton Electronics Division, p. 17.

VITA

Thomas Phillip Hertel was born on December 28, 1940 at Bourbon, Missouri. He received most of his primary and secondary education at Bourbon, Missouri. He received his college education at the University of Missouri - Rolla. He received a Bachelor of Science Degree in Electrical Engineering from the University of Missouri - Rolla in 1962.

He initially enrolled in the Graduate School of the University of Missouri - Rolla in January 1963 for one semester. He then returned to the Graduate School at the University of Missouri- Rolla for the school year of 1966-67 while teaching in the Electrical Engineering Department as assistant instructor.